Composite Structures 238 (2020) 111901

Contents lists available at ScienceDirect

Composite Structures

journal homepage: www.elsevier.com/locate/compstruct

Extension twist deformation response of an auxetic cylindrical structure inspired by deformed cell ligaments

David T. Farrell*, Conor McGinn, Gareth J. Bennett

Trinity College Dublin, The University of Dublin, Department of Mechanical and Manufacturing Engineering, D02 PN40, Ireland

ARTICLE INFO

Keywords:
Auxetic
Deformed ligaments
Axial rotation
EIT
Extension-twist

ABSTRACT

Recent advances in artificial metamaterials have allowed unique structures to deform in distinct modes not previously found in traditional material form. Auxetic structures that induce twist through deformation have been a focus of recent research. In this paper a cell-based tubular structure with pre-deformed ligaments is proposed which exhibits efficient extension induced twist (EIT) without the limitations of buckling. An analytical model of the structure is proposed using cell parameters to characterize the non-linear twist-deformation relationship. Samples of the structure were fabricated using the Ultimaker 3 platform with elastomer based TPU 95a build material and PVA support material. The analytical model and FEM were validated by tensile experiments, where fabricated samples reached 60 degrees of non-linear axial twist over 40 mm of deformation. In order to further characterize the structure's twist response, key design parameters of the lattice structure were varied and modelled. Actuation through tensile elastic deformation has key advantages in reliability and reduced complexity. Due to these advantages, this technology has potential applications in aerospace, biomedical and robotic fields.

1. Introduction

Fuelled by rapid advances in additive manufacturing, mechanical metamaterials have recently been exploited to generate unique modes of deformation and motion [1,2]. Deriving their properties through geometry, mechanical metamaterials have a unique level of application specific customization through variation of design parameters [3,4].

Auxetic structures are a class of metamaterial that exhibit Negative Poisson's Ratio [5]. First described by Love in 1944 [6], auxetics expand in the lateral direction under uniaxial loading. Auxetics exhibit unique mechanical properties such as energy dissipation [7,8] and deformation conversion modes [9,10]. Research into auxetics have used various types of artificial cells including: re-entrant, rotating-unit. and chiral structures [11]. Chirality and chiral structures have played a big role in creating micro- and macro-modes of deformation [12]. Chiral is defined as a shape which cannot be mapped onto its own mirror image by rotations or translations alone [13,14]. Due to their unique mechanical properties, chiral structures can be found throughout nature in DNA, plant tendrils, and proteins [15–17]. Artificial chiral cells in research have generally consisted of a central node surrounded by slender ligaments. Cells are classified by tri-, tetra-, and hexa-chiral structures, depending on the number of ligaments attached to a central node [11]. Chiral cell deformation can occur either through coupled response of node rotation and ligament deformation, or purely through ligament deformation [18].

In late 2017, Frenzel et al. proposed a 3D chiral cubic structure that exhibited induced twisted under compression [19]. The cube twisted axially through chiral node rotation and ligament deformation. The torsion generated in the proposed structure was dependent on the cell configuration and parameters. Li et al. later proposed a series of shear-compression coupling 3D metamaterials that exhibited the compression-induced-twisting effect (CIT) [20]. Topology optimization has also been used to generate similar torsional twist in designed structures [21]. Chen et al. [22] used topology optimization to generate bi-directional twist chirality in both tubes and beams. The tubular structure generated by Chen's optimization was quasi helical in nature. Wu et al. [23] proposed a rolled tetrachiral tube that exhibited CIT in a similar rotational response, inspired by the biomechanical process of a climbing chiral plant tendril and twisting leaf growth [16]. The proposed structure used pure sigmoidal ligament deformation to generate the twist, with a near linear relationship between the twist and vertical displacement. Ma et al. later expanded the theory behind rolled tetrachiral tube by proposing a theoretical model and verifying results through experimentation and FEM analysis [24]. Through the model proposed by Ma, the rotation generated by the structure was largely independent of the parent material properties [25]. It was also found

* Corresponding author.
E-mail addresses: farred10@tcd.ie (D.T. Farrell), mcginnc@tcd.ie (C. McGinn), gareth.bennett@tcd.ie (G.J. Bennett).

https://doi.org/10.1016/j.compstruct.2020.111901
Received 2 August 2019; Received in revised form 21 November 2019; Accepted 7 January 2020
Available online 21 January 2020

that localized buckling was the main mode of failure for the rolled chiral structure at higher displacements [26]. An extension-induced-twist (EIT) structure could avoid these buckling based limitations, allowing for larger degrees of twist. Lipton et al. [27] developed handed shearing auxetics (HSA's) that exhibited an extension-induced-twisting effect (EIT). These quasi helical structures were used by Chin et al. to develop a compliant grabber tool for recycling separation [28,29]. The gripper reversed the inputs of load induced twist, where axial displacement was generated by generating twist with an electric motor. Jopek et al. [30] investigated the torsion effects of a helical shaped composite bar, relating increase and decrease in elastic strain energy to helical pitch and material relationships.

This paper seeks to describe an investigation into auxetic cell structures that exhibit an extension included twist response, with a focus for future mechanical actuator development. By avoiding the limitations of compressive buckling, the focus of this proposed structure will be on achieving high angles of controlled induced twist using an elastomer-based material. The twist will also be characterized using a quasi-analytical model and FEM analysis, both of which could save time during the development of these structures by avoiding the tedious task of trial-and-error experimentation [10].

2. Auxetic deformation mechanisms

2.1. Initial supported buckling analysis

Before presentation of the proposed new structure, it is useful to provide initial context to the cell development for better understanding. The initial investigation was centered around chiral based twist-structure, first proposed by Wu et al. [23] and work by Ma et al. [25]. The rolled chiral cylinder structure showed strong potential for development as a mechanical actuator due to a hollow cylindrical shape and near linear twist deformation relationships. However, the CIT structure was restricted by a low threshold for buckling failure, limiting the maximum twist that a rotational actuator could achieve. An analysis of buckling was carried out using the finite element software ABAQUS. Structures were constructed and simulated using a similar method to Ma et al. [25]. As expected, the rolled chiral structure failed through localized buckling as seen in Fig. 1(a). An idea was proposed, that if an internal cylindrical support was placed inside the tube, the support could help the structure to continue rotation after buckling. Initial investigations of a "supported" compression were simulated in ABAQUS and shown in Fig. 1(b). The twist deformation response (ω/S_y) alongside Fig. 1 for both structures. As the structure continued to deform past the point of buckling, a stacked cell structure formed. During initial deformation, all structure ligaments compressed in unison; however, as the structure collapsed further individual ligaments collapse causing an erratic twist-response, as highlighted in the graph of Fig. 1. An investigation was carried out into designing a pre-deformed chiral cell, with collapsed ligaments, as seen in the FEM analysis. The theory stipulates that this structure would exhibit an extension-twist response (EIT) and avoid the limitations of compression-buckling.

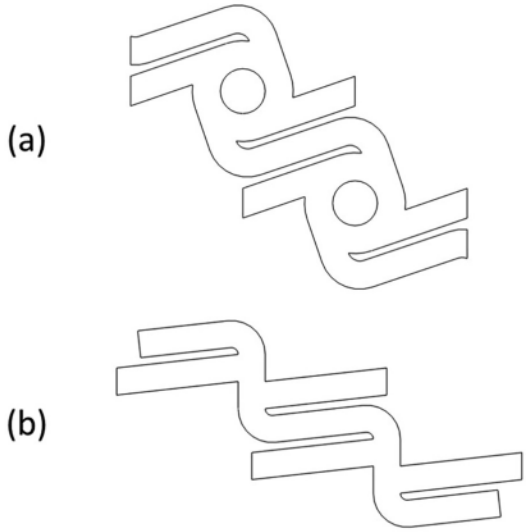

Fig. 2. (a) Replication of collapsed structure, (b) Improved cell without central node.

An initial design of the collapsed structure was developed in SolidWorks to replicate the structure seen in the FEA with a supported internal cylinder. The design developed is shown in Fig. 2(a). Due to the nature of pure bent ligament deformation, the circular node no longer determines the initial ligament angle. An improved cell design was then

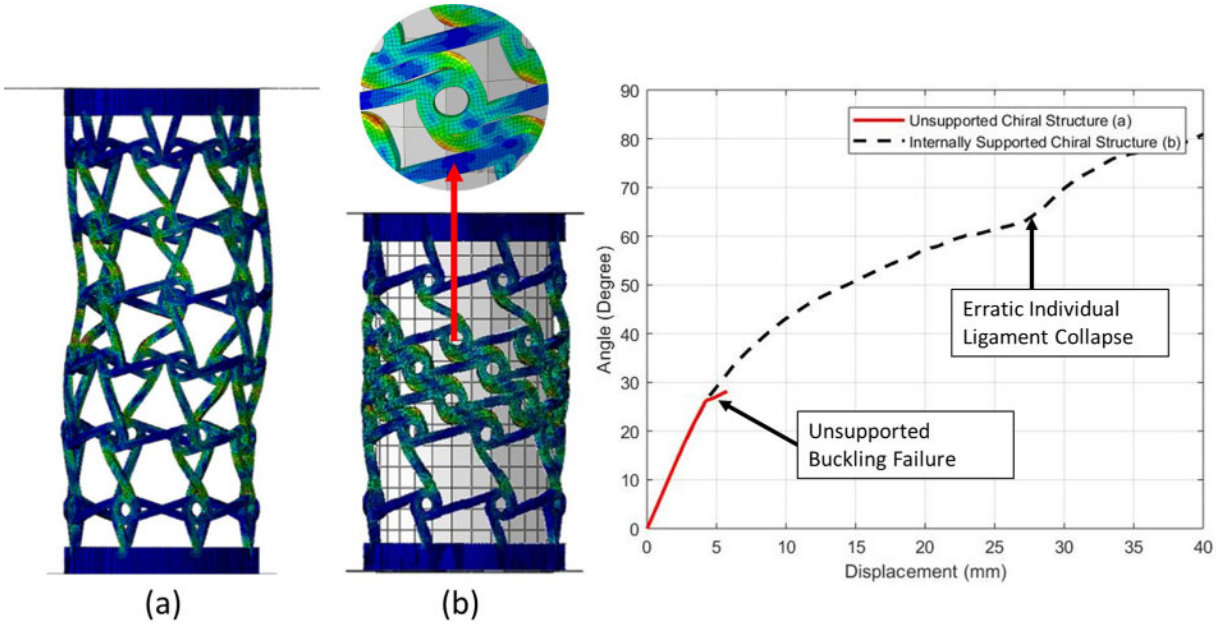

Fig. 1. (a) Buckling chiral structure under compression, (b) Internally supported chiral structure resisting buckling, with graph of twist-displacement relationship for both structures.

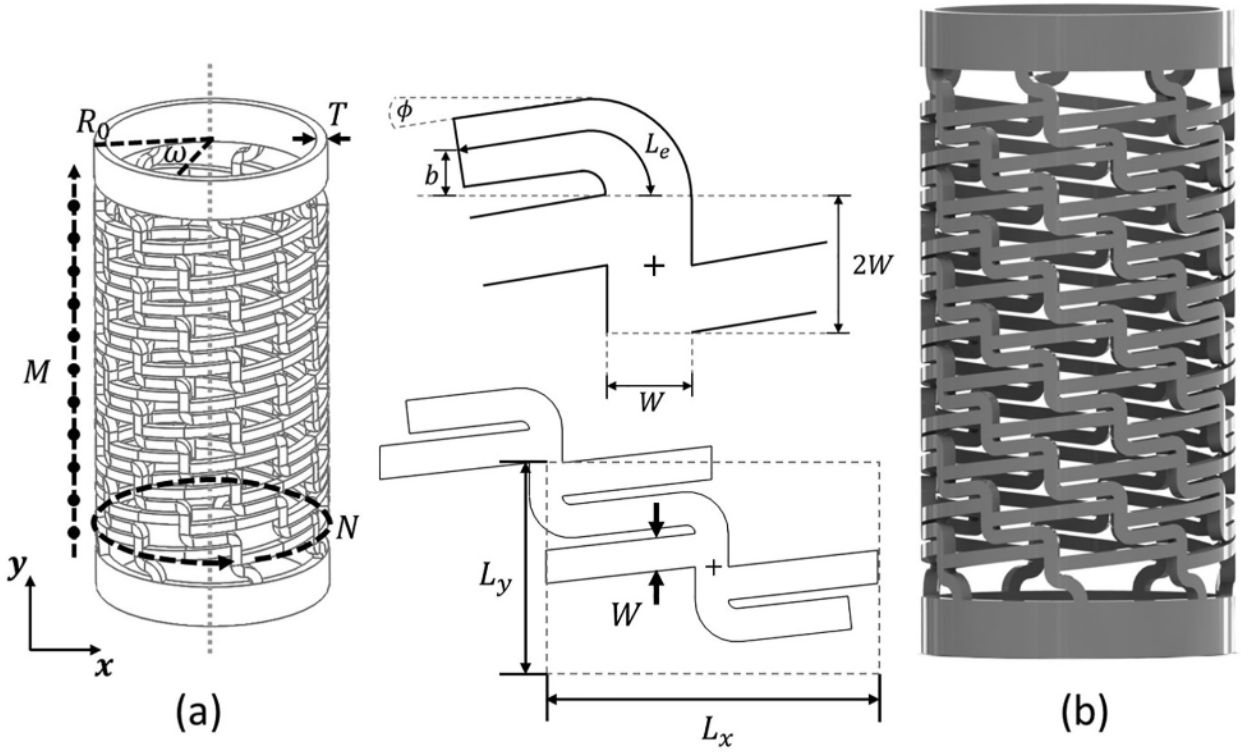

Fig. 3. (a) Schematics and parameters for extension induced structure (EIT), (b) Proposed design of EIT structure.

developed is shown in Fig. 2(b) without the circular node. These improvements allow for longer effective ligament lengths.

2.2. Proposed extension induced twist structure

Using the proposed pre-deformed cell, a rolled cylindrical shell was designed with the parameters shown in Fig. 3(a), where: M is the number of longitudinal cells (both in line and offset); N is the number of lateral cells around the shell; ω is the angle of axial twist of the structure; R_0 is the cylinder radius; T is the thickness of the cylinder. In terms of the cell design as described in Fig. 3, the basic cell outline can be defined by an L_xL_y rectangle. The overlapping design calls for each subsequent layer of longitudinal cells to be offset by $L_y/2$ in the y-direction, and $L_x/2$ in the x-direction. The central node is a $2WW$ rectangle, as seen in Fig. 3. The end of the ligament is placed at a height 'b' above the top of the node. The straight section at the end of the deformed ligament, is given at angle ϕ. The curve of the ligament is constructed as tangential to both the central node vertical sides and the straight section of the ligament at angle ϕ. L_e is a length taken along the whole deformed ligament including the length of the curve.

Fig. 3(b) shows a base design for an EIT structure designed in SolidWorks. The structure shown in Fig. 3(b) was designed with the parameters shown in Table 1. First, a flat cell was drawn and then patterned to create the lattice structure. A planar surface was then created from this lattice and connected using the knit tool, this generated pre-partitioned cells for the FEM analysis. Finally, the flat planar surface could be rolled into a tube using the flex feature.

Table 1
Structure parameters for extension induced twist design.

M	N	T	L_y	L_x	W	L_e	b
11	8	2 mm	12.5	20	2 mm	5.8 mm	1.13 mm

3. Method of twist characterization

3.1. Analytical model

The analytical model proposed is an approximate starting point to categorize the twist-deformation relationship using cell parameters (ligament length etc.). The design process would therefore consist of the initial analytical calculations, CAD, FEA, fabrication, and then experimentation. The model in this design process can be used to inform the design of a lattice structure to suit the actuator requirements. Analytical models for the twist-deformation analysis will use similar methods to that found in literature [13,25] derived from Euler beam theory. The ligament is modelled in reverse, under the assumption that at max extension ($S_{y,max}$) the beam is near straight and vertical. The model will ignore the displacement effects due to strain to reduce complexity. The twist derivative in the x- and y-directions is given by Eqs. (2) and (1), where 'a' is the local axis of the ligament along the length L_e.

$$\frac{dS_x}{da} = \frac{6L_e^2 F sin(\theta)}{E_s z W^3} cos(\theta) \tag{1}$$

$$\frac{dS_y}{da} = -\frac{6L_e^2 F sin(\theta)}{E_s z W^3} sin(\theta) \tag{2}$$

where: L_e is the characteristic length, F is the applied force, z is the depth of the ligament, W is the thickness of the ligament, and E_s is the Young's Modulus of the parent material. In this analytical model is varied as the theoretical angle of the overall ligament. However, when deformed the ligament will include both straight and curved sections. Therefore, the initial angle of θ proved difficult to determine due to this deformation of the ligament shape. The model used in this paper estimated the initial overall θ using geometric parameters. The solution assumes that length 'b', the length between the tip of the ligament and the top of the node (as shown in Fig. 3), was sufficiently small. If 'b' is small, we know that in the model, if 'b' is equal to zero the angle θ will also equal zero. θ is approximated in Eq. (3).

$$\theta \approx (b/L_e)90° \tag{3}$$

As an approximation, the reasoning behind this model choice of θ stems from the purpose of the analytical model. In the design process, given structure requirements for a twist-deformation relationship, the analytical model gives an easy approximation for this relationship before more lengthy analysis of FEM and experimentation.

Due to the large deformation, the equations will use a numerical method to solve for the twist at a given displacement. Using MATLAB and equations above the twist derivative will be calculated by iterating over small perturbations ($dS_y = 0.01$). The equation for the twist derivative, derived from Eqs. (1) and (2), is shown in Eq. (4).

$$\frac{d\omega}{dS_y} = \frac{cos(\theta)}{R_0 sin(\theta)} \tag{4}$$

The derivative is then used to calculate the change in twist-deformation relationship over a small displacement for the whole structure, as shown in Eq. (5).

$$\omega_1 = \omega_0 + 2MdS_y \frac{d\omega}{dS_y} \tag{5}$$

where; 2M calculates the displacements over the number of full vertical ligaments in the geometrical shape. Using the model in MATLAB, an approximate relationship between twist and displacement can be established for given cell parameters before the CAD process. The results from analytical model will be compared to FEM analysis and experimental results in the following sections.

3.2. Finite element modelling

The rotation response of the EIT structure was simulated based on a method outlined by Ma et al. [24,25]. For the FEM analysis an academic version of ABAQUS FEA software was used. The model used a dynamic explicit solver along with material properties for TPU 95a obtained from Ultimaker Guidelines [31]. The 8-node linear brick with reduced integration and hourglass control (C3D8R) element type was used for increased accuracy and speed. The chiral structure was pre-partitioned in SolidWorks and imported as a surface feature into ABAQUS. The surface was then meshed, creating a uniform and high quality mesh of hexahedral elements (as seen in Fig. 4). The mesh is then extruded in ABAQUS to retain the uniformity of the mesh structure across the thickness of the tube. The model placed the meshed chiral structure between two shell plates, with a fixed bottom plate (ENCASTRE) and a constrained top plate that could allow rotation and axial movement (U_y and UR_y).

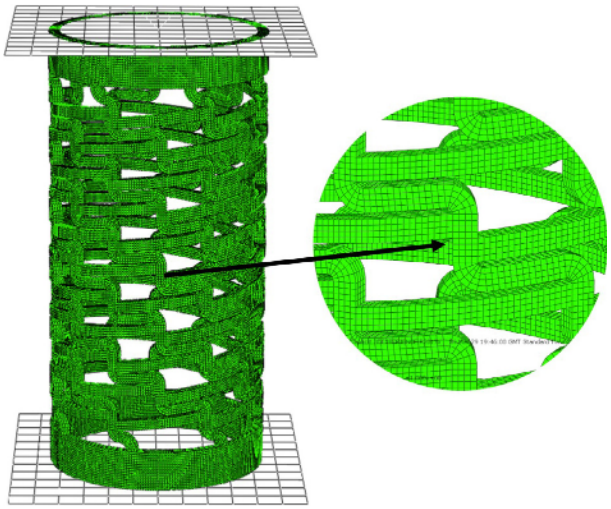

Fig. 4. Meshing of test sample for FEM.

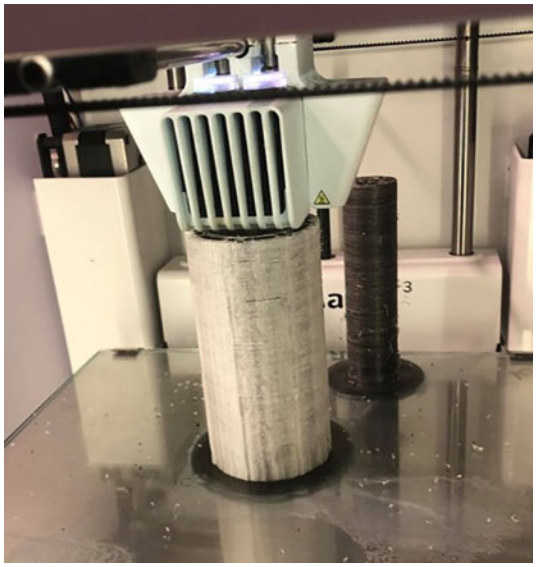

Fig. 5. Fabrication on Ultimaker 3 platform with TPU Material (black) and PVA water soluble support (white).

3.3. Fabrication and experimentation

To validate both the theoretical and simulation results, samples of the EIT structure were fabricated and testing using the following methods.

The EIT structure was fabricated using TPU 95a on the Ultimaker 3 platform. The flexible and elastic properties of TPU 95a allowed the structure to reach higher deformations of twist. The sample was fabricated using PVA support material that allowed the printer to generate the complex EIT structure, as seen in Fig. 5. The PVA material was water-soluble and could be easily removed in post-processing.

Fabricated samples were then tested on an Instron 3366 universal testing machine. The Instron recorded the force and linear displacement, while the angle was measured using a needle attached to the bottom of the EIT structure and a protractor (with an accuracy of ± 0.5°). The angle was recorded by a camera placed above the needle, as in the set-up shown in Fig. 6(a).

As the Instron machine applied tensile load, the structure deformed causing the EIT structure to rotate axially, as shown in Fig. 6. To generate the required boundary conditions, a pinned clamp was attached to the top of the structure. The bottom boundary conditions are constrained by the components shown in Fig. 6(c). The components consisted of a thrust bearing inside a clamp that is attached to the inside of the cylindrical structure. The attachment relied on friction and small protruding notches to remain connected to the structure. A retaining bolt restricted the linear deformation of the structure, while the thrust bearing allowed for near frictionless axial rotation.

4. Results

4.1. Validations of characterization methods

The results between the analytical model, FEM analysis, and experimentation methods of characterization are shown in Fig. 7, conducted on a sample with identical parameters from Table 1. The experiment was conducted on the Instron 3366, with a protractor angle accuracy of ± 0.5°. As seen in Fig. 7, the experimental results validate and agree with both the FEM analysis and analytical model. The analytical model proved to be a good approximation for the twist response given the assumptions and approximations in ligament parameters. The results for all methods show a non-linear relationship in the twist response, with the twist derivative (deg/mm) gradually increasing at

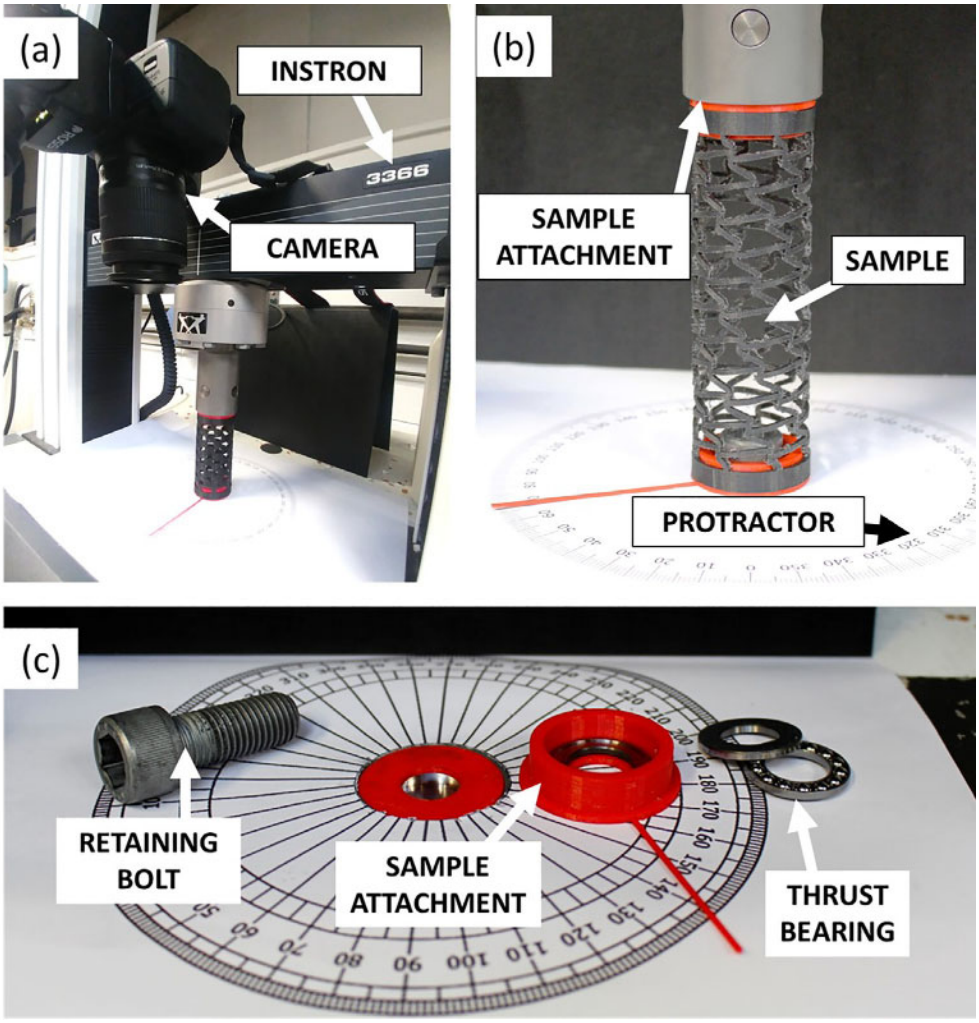

Fig. 6. (a) Experimental set-up for testing extension induced twist structures, (b) Close-up of sample attachment and needle-protractor set-up, (c) Attachment components.

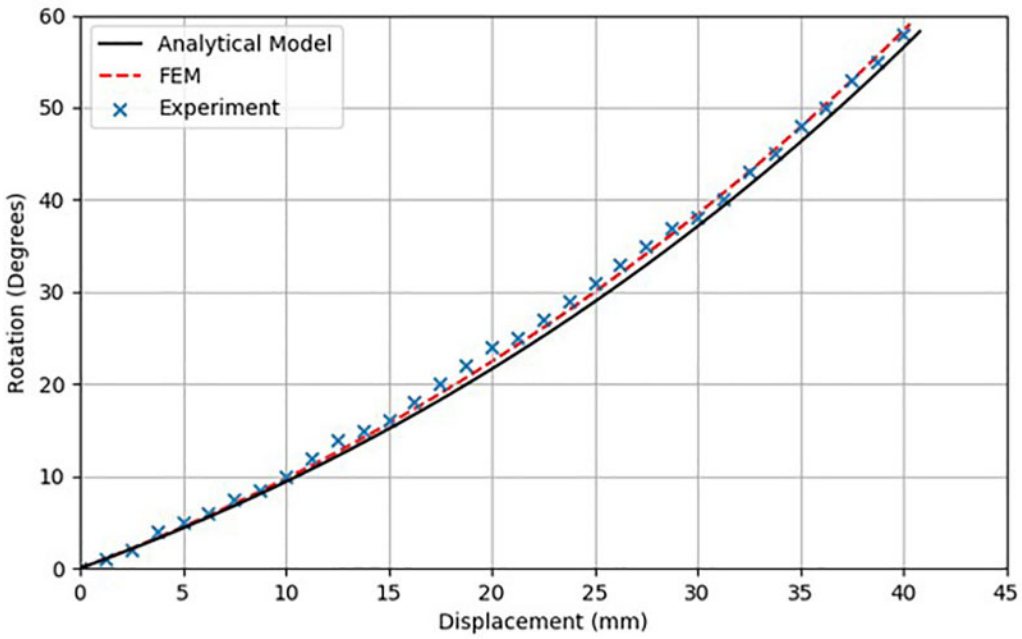

Fig. 7. Comparison of twist and deformation between the analytical model, FEM analysis, and experimental results for structure described in Table 1.

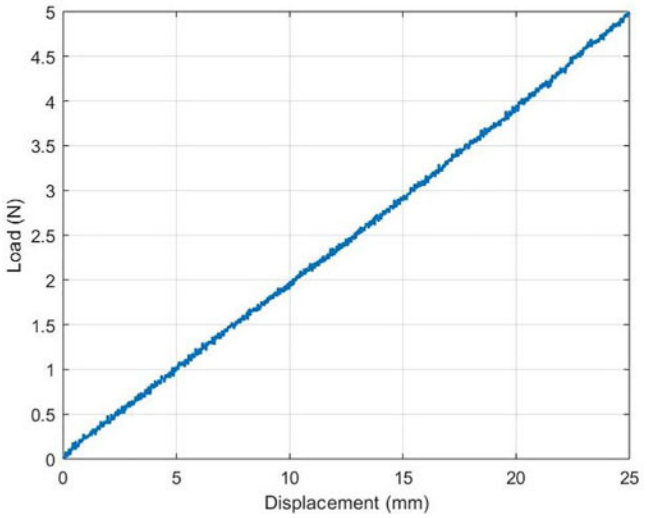

Fig. 8. Experimental results for force against displacement for EIT under extension loading.

larger displacements. The increase in the rate of twist comes from the increase in the ligament angle (θ), and the shortening of the x-component of the ligament, as seen in Eq. (4). The rate of twist increases from initially 1 deg/mm to 5 deg/mm at 40 mm of displacement. By generating the twist through extension, rather than compression, the structure can surpass the limitations of buckling and achieve higher angles of twist, up to 60° for 40 mm of displacement. The force response of the structure is somewhat linear with tensile deformation, as shown in Fig. 8.

The elastic TPU 95a material used in the fabrication of these structures allowed for the high levels of elastic deformation in the cell structure. Although not quantified in this work, the auxetic nature of the structure can be seen in Fig. 9. As longitudinal ligaments deform, generating twist, the lateral ligaments keep a near constant tube diameter. As the ligaments layers began to delaminate at around 60° of rotation and 9 Newtons of Force the twist became unpredictable. With

Fig. 9. Large deformation of ligaments under tensile load, at 42% strain.

validation of the characterization methods, subsequent analysis of structure parameters was conducted purely through FEM and analytical models to reduce time of the lengthy process of fabrication and experimentation.

4.2. The impact of lateral nodes

The lateral dimensions of the cylinder (L_x, R_0, and N) can all be expressed using the following relation based on the circumference length: $L_x = 2\pi R_0/N$. FEM and analytical analysis was conducted to understand how the twist relationship of the proposed structure changes depending on the number of lateral cells. Three different models of EIT structure were developed with similar parameters for ligament thickness, longitudinal node count, wall thickness, ligament length, and ligament angle.

Each structure varied in the number of lateral nodes from 6 nodes to 4 nodes, with identical cell dimensions and a decreasing cylinder radius for each node removed. The twist deformation response of the structures is shown in Fig. 10. With reduced lateral cells the rate of rotation with respect to linear displacement ($d\omega/dS_y$) increases. Results between the analytical and FEM methods appear to match in a similar relationship. There is a deviation of results with small lateral nodes (N = 4), this could be due higher individual ligament strains, something the analytical model does not take into account.

4.3. Theoretical cell parameters

To further understand the effect of the two key ligaments parameters of length (L_e) and angle (θ), an investigation using the analytical model to determine their effect on the twist response, and the rate of change of twist against displacement (dw/dS_y). Fig. 11 (a) shows the twist relationship with the ligament effective length L_e. As the ligament length increases relative twist response remains near constant. However; the rate of twist changes as higher deformations, as shown in the derivative graph Fig. 11(b). The derivative initially begins in the same location (0.8 deg/mm) but begins to diverge as the ligament deforms.

The ligament angle θ has more of an effect on the overall ligament deformation as shown in Fig. 12(a). The deviation in the twist-deformation relationship can be seen at small deformations with large differences in how the twist develops. The twist derivative relationship ($d\omega/dS_y$) shows the unique initial rate of twist for a given ligament angles θ.

5. Discussion

The twist-deformation relationship of the new proposed cell-based structure has been clearly defined in analytical, FEM, and experimental methods. Being able to define the structure with these separate models has key advantages in the actuator development process as it avoids the tedious task of trail-and-error experimentation is avoided. With a clearly defined twist-deformation mechanism, an actuator design using this structure could exhibit a high level of reliability and control.

Axial twist in response to applied load is not a new concept, it is observed in origami [32] and helical mechanical springs [33]. However, generating the twist using auxetic cells allows for the structures to retain their shape during bi-directional twist with minimal lateral contraction. Similar extension twist structures have been proposed in literature from Lipton [27] in the form of Handed Shearing Auxetics. In comparison to the proposed structure in this paper, the HSA's have long helical strands while this structure is comprised of much smaller ligaments. Both structures have application-specific advantages that could be explored in future research. Further controlability of the structures twist response could be explored using Composites and external factors e.g. temperature, magnetic field, similar to Jopek et al. [34].

Using extension-twist instead of compression-twist avoids the buckling failure seen in previous rolled chiral structures, allowing for

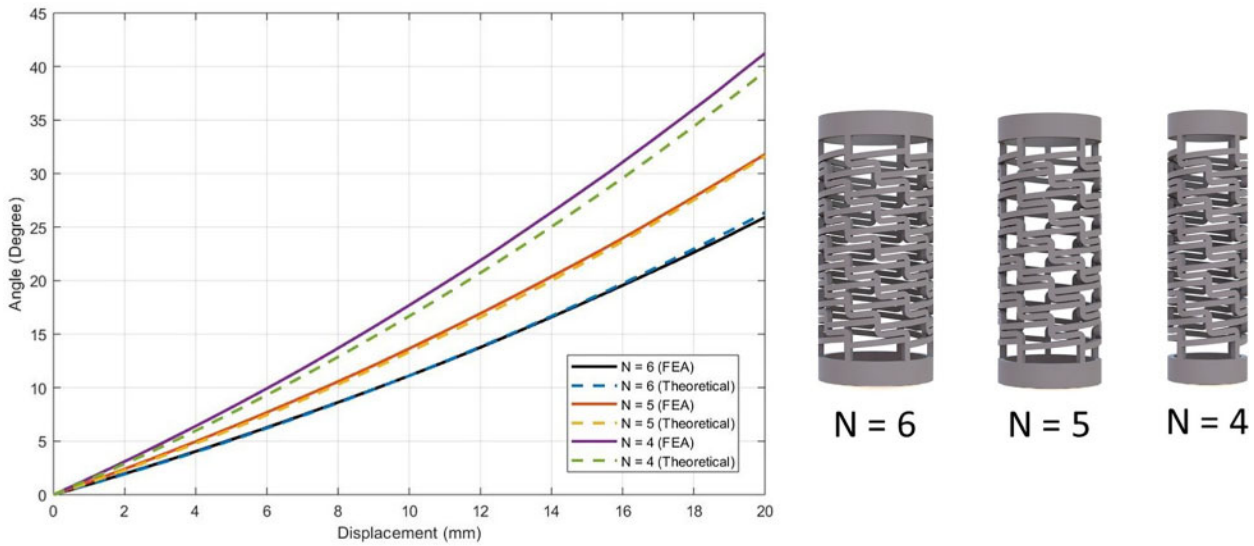

Fig. 10. Investigation on lateral cell numbers to twist-deformation response with constant cell parameters ($W = 2$ mm, $T = 2$ mm, $M = 11$).

higher degrees of twist and deformation. The new mode of failure occurs with fracture in individual ligaments. The highest stress concentration in the structure is located in the connection between node and ligaments. This is where the majority of bending action takes place, as seen in Fig. 10. Future developments for a mechanical actuator could attempt to reduce this stress and investigate the effect of fatigue on the structure after repeated rotations.

6. Conclusions

Based on the deformed structure of a compressed tetra-chiral tube, a cell-based extension induced twist auxetic structure was proposed. Characterization of the structures twist was investigated using an analytical model and FEM analysis, which were validated through experimental data using AM fabricated elastomer samples. The proposed structure exhibited efficient extension induced twist up to 60° of axial twist for 40 mm of displacement. Further analysis determined the effect of lateral node count and tubular diameter on the twist deformation relationship. The main conclusions from this research are as follows.

(1.) The extension induced twist of the proposed structure can be characterized accurately through an analytical model, FEM, and experimental methods.
(2.) The twisting response is non-linear but still highly controllable, with a low rate of change over large displacements. This twist response can be altered through variation of cell parameters, with a smaller tube radius achieving a higher twist per unit displacement.
(3.) With recent advancements in additive manufacturing and the use of elastomer based materials, this proposed structure shows potential for future mechanical actuator scenarios that require a reliable method of twist generation.
(4.) The proposed structure shows strong potential for a composite configuration, with stiff lateral ligaments and highly deformed longitudinal ligaments. Fabrication of composite samples could allow for higher achievable angles of twist with elastic material or increased lateral rigidity.

Author Disclosure Statement

No competing financial interest exist.

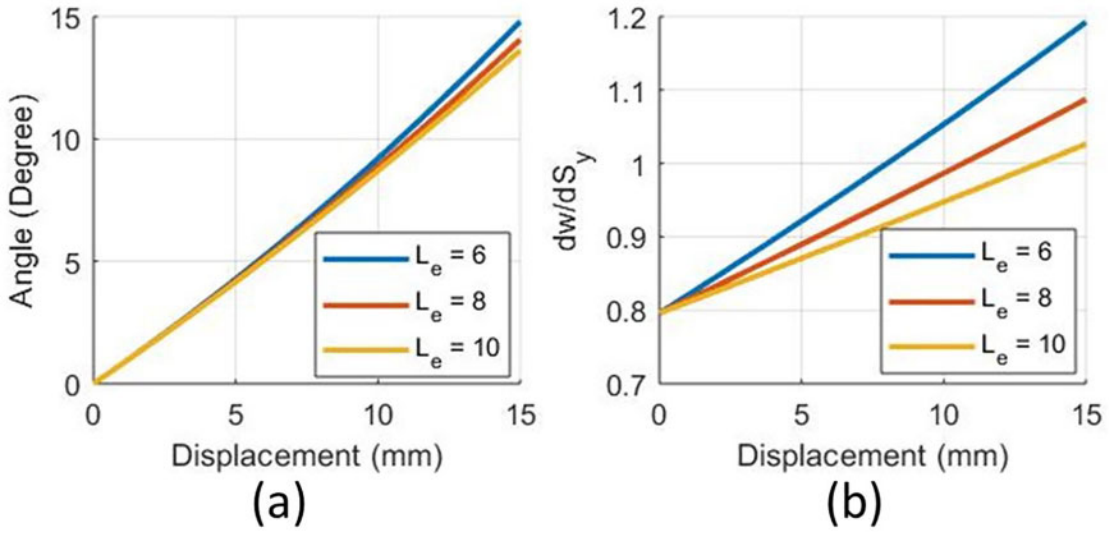

Fig. 11. Variations in ligament length (L_e in mm) and the effect on the rate of twist.

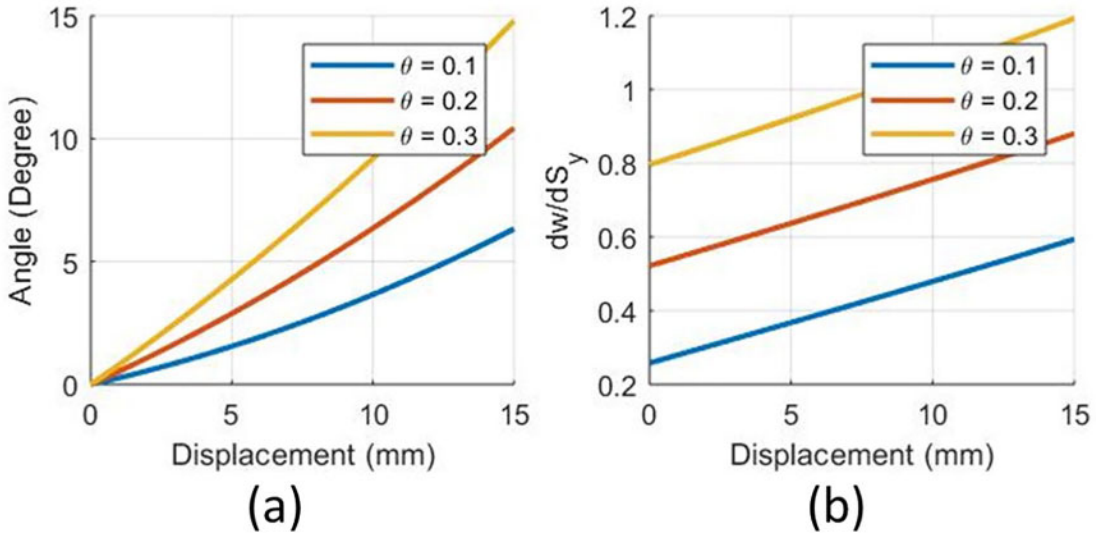

Fig. 12. Variations in ligament angle (θ) and the relationship to the initial twist response.

CRediT authorship contribution statement

David T. Farrell: Conceptualization, Methodology, Software, Validation, Formal analysis, Investigation, Resources, Writing - original draft, Writing - review & editing, Visualization. **Conor McGinn:** Conceptualization, Methodology, Resources, Writing - review & editing, Supervision. **Gareth J. Bennett:** Conceptualization, Methodology, Resources, Writing - review & editing, Visualization, Supervision, Project administration, Funding acquisition, Project Supervisor.

Declaration of Competing Interest

The authors declare that they have no known competing financial interests or personal relationships that could have appeared to influence the work reported in this paper.

Acknowledgements

The authors would like to acknowledge funding received from Trinity College Dublin, Dublin 2, Ireland.

Appendix A. Supplementary data

Supplementary data associated with this article can be found, in the online version, at https://doi.org/10.1016/j.compstruct.2020.111901.

References

[1] Bertoldi K, Vitelli V, Christensen J, van Hecke M. Flexible mechanical metamaterials. Nat Rev Mater 2017;2:17066.
[2] Florijn Bastiaan, Coulais Corentin, van Hecke Martin. Programmable mechanical metamaterials: the role of geometry1. Cambridge, England: Royal Society of Chemistry; 2016.
[3] Christensen Johan, Kadic Muamer, Kraft Oliver, Wegener Martin. Vibrant times for mechanical metamaterials, [New York]: Cambridge University Press for the Materials Research Society, 2015, 2015.
[4] Shufrin I, Pasternak E, Dyskin AV. Effective properties of layered auxetic hybrids. Compos Struct 2019;209:391–400.
[5] Kolken H, Zadpoor A. Auxetic mechanical metamaterials. RSC Adv 2017;7:5111–29.
[6] Love AEH. A treatise on the mathematical theory of elasticity. 4th ed. Cambridge: Cambridge University Press; 1927.
[7] Carneiro VH, Meireles J, Puga H. Auxetic materials – a review. Mater Sci-Poland 2013;31:561–71.
[8] Karathanasopoulos N, Reda H, Ganghoffer J-F. Designing two-dimensional metamaterials of controlled static and dynamic properties. Comput Mater Sci 2017;138:323–32.
[9] Lechenault F, Thiria B, Adda-Bedia M. Mechanical response of a creased sheet. Phys Rev Lett 2014;112.
[10] Fernandez-Corbaton I, Rockstuhl C, Ziemke P, Gumbsch P, Albiez A, Schwaiger R, Frenzel T, Kadic M, Wegener M, et al. New twists of 3d chiral metamaterials. Adv nced Mater 2019:1807742.
[11] Novak N, Vesenjak M, Ren Z. Auxetic cellular materials – a review. Strojniki vestnik J Mech Eng 2016;62:485–93.
[12] Coulais C. As the extension, so the twist. Science 2017;358:994–5.
[13] Fu M-H, Zheng B-B, Li W-H. A novel chiral three-dimensional material with negative Poisson-s ratio and the equivalent elastic parameters. Compos Struct 2017;176:442–8.
[14] Lorato A, Innocenti P, Scarpa F, Alderson A, Alderson K, Zied K, Ravirala N, Miller W, Smith C, Evans K. The transverse elastic properties of chiral honeycombs. Compos Sci Technol 2010;70:1057–63.
[15] Schäferling M. Chirality in nature and science. Chiral nanophotonics, vol. 205. Cham: Springer International Publishing; 2017. p. 5–42.
[16] Wang J-S, Wang G, Feng X-Q, Kitamura T, Kang Y-L, Yu S-W, Qin Q-H. Hierarchical chirality transfer in the growth of Towel Gourd tendrils. Scientific Rep 2013;3.
[17] Zhao Z-L, Zhao H-P, Li B-W, Nie B-D, Feng X-Q, Gao H. Biomechanical tactics of chiral growth in emergent aquatic macrophytes. Scientific Rep 2015;5:12610.
[18] Prall D, Lakes RS. Properties of a chiral honeycomb with a poisson's ratio of - 1. Int J Mech Sci 1997;39:305–14.
[19] Frenzel T, Kadic M, Wegener M. Three-dimensional mechanical metamaterials with a twist. Science 2017;358:1072–4.
[20] Li X, Yang Z, Lu Z. Design 3d metamaterials with compression-induced-twisting characteristics using shear-compression coupling effects. Extreme Mech Lett 2019;29:100471.
[21] Zhang H, Luo Y, Kang Z. Bi-material microstructural design of chiral auxetic metamaterials using topology optimization. Compos Struct 2018;195:232–48.
[22] Chen W, Ruan D, Huang X. Optimization for twist chirality of structural materials induced by axial strain. Mater Today Commun 2018;15:175–84.
[23] Wu W, Geng L, Niu Y, Qi D, Cui X, Fang D. Compression twist deformation of novel tetrachiral architected cylindrical tube inspired by towel gourd tendrils. Extreme Mech Lett 2018;20:104–11.
[24] Ma C, Lei H, Liang J, Wu W, Wang T, Fang D. Macroscopic mechanical response of chiral-type cylindrical metastructures under axial compression loading. Mater Design 2018;158:198–212.
[25] Ma C, Lei H, Hua J, Bai Y, Liang J, Fang D. Experimental and simulation investigation of the reversible bi-directional twisting response of tetra-chiral cylindrical shells. Compos Struct 2018;203:142–52.
[26] Zheng B-B, Zhong R-C, Chen X, Fu M-H, Hu L-L. A novel metamaterial with tension-torsion coupling effect. Mater Design 2019;171:107700.
[27] Lipton JI, MacCurdy R, Manchester Z, Chin L, Cellucci D, Rus D. Handedness in shearing auxetics creates rigid and compliant structures. Science 2018;360:632–5.
[28] Chin L, Yuen MC, Lipton J, Trueba LH, Kramer-Bottiglio R, Rus D. A simple electric soft robotic gripper with high-deformation haptic feedback 7.
[29] Chin L, Lipton J, Yuen MC, Kramer-Bottiglio R, Rus D. Automated recycling separation enabled by soft robotic material Classinücation 6.
[30] Jopek H, Strek T. Torsion of a two-phased composite bar with helical distribution of constituents. Physica Status Solidi (b) 2017;254:1700050.
[31] Ultimaker. TPU Material Properties Guide; 2018.
[32] Nayakanti N, Tawfick SH, Hart AJ. Twist-coupled Kirigami cells and mechanisms. Extreme Mech Lett 2018;21:17–24.
[33] Wahl AM. Mechanical springs, number xi, 435 p. in [Machine design series]: Penton Pub. Co., Cleveland, O.; 1944.
[34] Jopek H. Finite element analysis of tunable composite tubes reinforced with auxetic structures. Materials 2017;10.